Biomechanics of Stretch-Induced Beading

Vladislav S. Markin,* Darrell L. Tanelian,* Ralph A. Jersild, Jr.,# and Sidney Ochs§

*Departments of Anesthesiology and Pain Management and Biomedical Engineering, University of Texas Southwestern Medical Center, Dallas, Texas 75235-9068; and #Department of Anatomy and §Department of Physiology and Biophysics, Indiana University School of Medicine, Indianapolis, Indiana 46202 USA

ABSTRACT To account for the beading of myelinated fibers, and axons of unmyelinated nerve fibers as well of neurites of cultured dorsal root ganglia caused by mild stretching, a model is presented. In this model, membrane tension and hydrostatic pressure are the basic factors responsible for axonal constriction, which causes the movement of axonal fluid from the constricted regions into the adjoining axon, there giving rise to the beading expansions. Beading ranges from a mild undulation, with the smallest degree of stretch, to more globular expansions and narrow intervening constrictions as stretch is increased: the degree of constriction is physically limited by the compaction of the cytoskeleton within the axons. The model is a general one, encompassing the possibility that the membrane skeleton, composed mainly of spectrin and actin associated with the inner face of the axolemma, could be involved in bringing about the constrictions and beading.

INTRODUCTION

Varicosity formation or the beading of nerve fibers and cultured neurites has been commonly regarded to be a sign of neural abnormality: a metabolic perturbation, mechanical trauma, aging, or the action of a neurotoxic agent (Ochs et al., 1997). However, it is seen in the fibers of normal nerves when they are mildly stretched and rapidly fixed by freeze-substitution or cold fixation (Ochs and Jersild, 1987), with recent evidence also indicating that beading may be a normal process in neurites *in vivo*, occurring as a result of nervous system activity (Allen et al., 1997; Zhu et al., 1997). Electrical stimulation of the sensory afferents of mice or application of capsaicin to their peripheral nerves result in the release of substance P from afferent terminals in the spinal cord synapsing onto apical dendrites in the dorsal horn cells, causing them to become temporarily beaded—beading occurs quickly and then is reversed within an hour (Mantyh et al., 1995). Similar beading is seen when substance P is applied to dorsal root ganglion (DRG) neurons in culture (Tanelian and Markin, 1997). Beading in these cases was assumed to be due to the internalization of substance P membrane receptors within the dendrites (Mantyh et al., 1995; Tanelian and Markin, 1997). However, beading also occurs in neurites of normal cultured DRG neurons when they are stretched (Tanelian and Markin, 1997). Stretching by means of a patch-clamp electrode applied to a neuronal process results in the neurites quickly taking on a beaded form and resuming their cylindrical form after relaxation.

Pure lipid bilayer tubes can demonstrate a beaded form change with application of laser-induced mechanical force, suggesting that only lipid is required for beading (Bar-Ziv and Moses, 1994). However, there is an array of nerve fiber form changes that develops with increasing stretch, ranging from a mild sinusoidal undulation to a series of globular regions with longer narrow constrictions between them (Pourmand et al., 1994). Unlike the smooth undulations of the beaded axons of the unmyelinated fibers in stretched nerves, the beaded myelinated fibers show regional differences. The greatest degree of beading is seen in the middle part of the internodes, with relatively long lengths of the internodes adjoining the nodes remaining unbeaded (Ochs et al., 1994). These variations along the length of the fiber, plus the intrusions seen in the constrictions, led to the concept that the membrane skeleton associated with the lipid bilayer plays an active role in beading (Ochs et al., 1996, 1997). In the constrictions of the fibers showing beading, the cytoskeleton becomes tightly compacted, and the compacted cytoskeleton imposes a limit on further constriction. When the cytoskeleton is degradated by β,β'-iminodiproprionitrile (IDPN), beading remains and is even enhanced, indicating that the cytoskeleton is not essential for beading, and the beading of axons indicates that beading is a property associated with the axolemma (Ochs et al., 1996).

Previously, beading was analyzed by using a model in which the neuronal membrane surface area was considered to be reduced and beading resulted from the necessary redistribution of membrane bilayers, which were free to rearrange because of cytoskeletal disaggregation (Tanelian and Markin, 1997). The final shape was approximated by a combination of spheres and cylinders.

The major drawback of the previous model was that it did not calculate the actual shape of a beaded fiber, but rather postulated it. To take into account the wide range of properties ascribed to beading and the variation in the degree of beading and compaction of the cytoskeleton within the

Received for publication 25 November 1998 and in final form 2 February 1999.

Address reprint requests to Dr. Vladislav S. Markin, Department of Anesthesiology and Pain Management, University of Texas Southwestern Medical Center, 5323 Harry Hines Blvd., Dallas, TX 75235-9068. Tel.: 214-648-5632; Fax: 214-648-2229; E-mail: markin@utsw.swmed.edu.

0006-3495/99/05/2852/09 $2.00

constrictions in different nerve fiber types (Ochs et al., 1997), including reports of bead-like form changes in neurites, a new model is presented here that can predict the shape of a fiber and universally describe beading. This model can account for beading on the basis of the axonal membrane being free to undergo deformation under the influence of tension and hydrostatic pressure, with the membrane skeleton intimately conjoined with the lipid bilayer (as earlier described for the erythrocyte by Elgsaeter et al., 1986).

OBSERVATIONS OF THE BEADED FORM

Studies of beading were carried out on cat and rat sciatic nerves. Beads were first seen in nerves when prepared by freeze-substitution (Ochs and Jersild, 1987). In brief, nerves were rapidly frozen while under stretch by immersing them in stirred Freon-12 cooled with liquid nitrogen to a temperature close to −160°C. The frozen segments were freeze-substituted with osmium tetroxide in acetone and then prepared for light microscopy or electron microscopy. Furthermore, nerves under stretch were cold-fixed by glutaraldehyde fixation at a temperature close to 0°C, a method that also preserves most of the beading (Ochs et al., 1994). Nerves prepared by either fixation technique were sectioned for microscopy, or individual fibers were teased from the fixed preparation to observe form variation along their length.

In the axons of unmyelinated fibers, a succession of expansions and constrictions can be seen (Fig. 1) that looks like the beading of neurites. These are similar to the succession of beading enlargements and constrictions seen in myelinated fibers, although there are regional differences within the internodes (Fig. 2). In this figure of a single myelinated fiber isolated by teasing, the degree of beading, as typically found, is greatest around in the internode close to the midpoint of the fiber, where the Schwann cell nucleus is present (Ochs et al., 1994). As is typical for beaded myelinated fibers, the region of the internode for some distance around the nodes shows little or no beading. Intrusions are seen as small dark-staining protuberances projecting into the axon from the inner wall of the myelin sheath (Ochs and Jersild, 1990).

Within the compacted constrictions of the beaded fiber, the cytoskeletal organelles, microtubules, and neurofilaments are much more closely apposed than normally (Fig. 3). Associated with the beaded fibers are intrusions into the axon, which may be seen as hillocks containing lamellae arising from the inner wall of the myelin sheath. These are covered with axolemma, which also show a degree of wrinkling. The various forms of the intrusions suggest a progression of such intrusive forms from finger-shaped light-

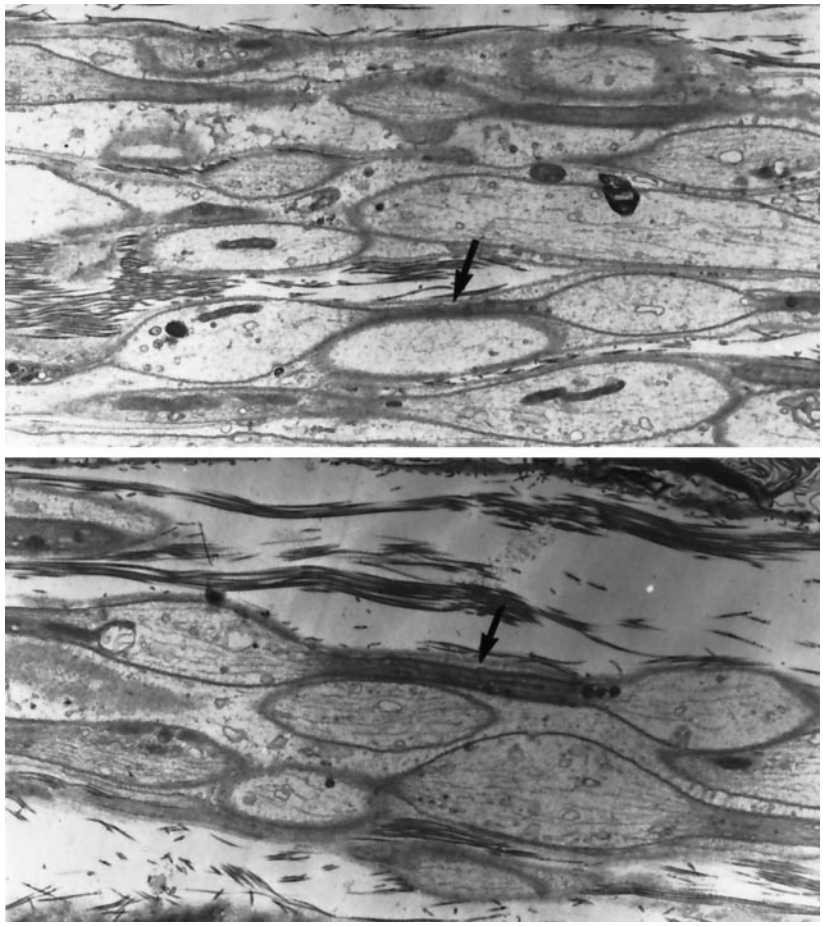

FIGURE 1 Beaded axons in unmyelinated fibers. A succession of expansions and constrictions can be seen within the axons of these longitudinally sectioned unmyelinated fibers in EM. Note the compacted cytoskeleton within the constrictions (*arrow*), causing them to appear as a dark-stained band. Magnification ×11,000.

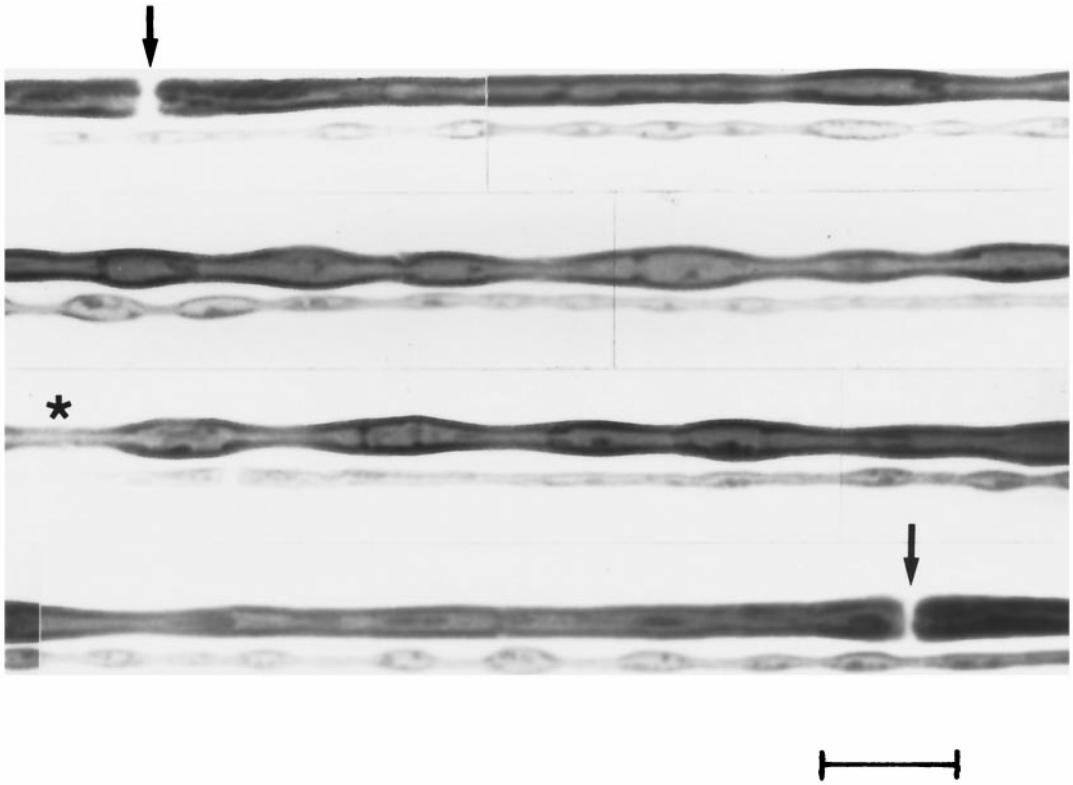

FIGURE 2 A single myelinated fiber teased from a rat sciatic nerve stretched with a weight of 4.5 g to bead its fibers and cold-fixed while remaining under stretch. The fiber teased from the nerve shows a high degree of beading, which typically is greatest in the internode around the midpoint of the fiber (asterisk) where the Schwann cell nucleus is generally found. In this particular fiber beading is more asymmetrical than usual, with more beading seen to one side of the internode than the other (cf. Ochs et al., 1994). As is typical, the region of the internode for some distance around the nodes (*arrows*) shows no beading. Intrusions are seen as small dark-staining protuberances projecting into the axon from the inner wall of the myelin sheath. These are to be differentiated from the dark-staining region crossing the fiber, which represents an incisure of Schmitt-Lantermann. Bar = 50 μm.

staining intrusions with little associated lamellae, to the hillocks and spheres with clearly defined lamellae in them, similar to that of the parent myelin sheath (Ochs and Jersild, 1990).

THEORETICAL

Model

We assume that a fiber is a cylinder with a fluid membrane, so that it can easily change its shape within the constraints of constant membrane area and fiber volume. The stretching force applied to the fiber causes tension in the membrane and, hence, creates hydrostatic pressure in the cytoplasm. A fluid cylinder with surface tension is known to be unstable. Therefore it will change its shape, provided the length of the cylinder is increased (Fig. 4). If the membrane is fluid, homogeneous, and isotropic and is not supported by the cytoskeleton, its tension (γ) determines the transmembrane pressure differential (p) according to the Laplace equation:

$$p = \gamma(c_p + c_m). \quad (1)$$

Here c_p and c_m designate the principle curvatures of the membrane.

However, it was found for myelinated fibers (Ochs and Jersild, 1987) and for axons of unmyelinated fibers (Ochs et al., 1996; Fig. 2) that in the constricted regions of the nerve fiber, the cytoskeleton is not depolymerized but rather becomes compressed into a tight core of closely packed cytoskeletal organelles, with further constriction checked by this core. Therefore, the transformed nerve fiber can consist of alternating beading expansions and supported cylindrical constrictions (Fig. 5). Mechanical equilibrium in beads is determined by the Laplace equation, and the cylindrical part of the transformed nerve fiber rests on the core and has a radius equal to the minimum radius of the bead. The cylindrical region has a larger mean curvature than the beaded region, and they are under the same tension. That means that the membrane over the cylindrical region should produce higher pressure, but an opposing pressure created by the cytoskeleton core when it is compacted counters this excessive pressure. The two forms *smoothly* transform into each other.

Two or more beads can be located next to each other as in Fig. 4, or they can be separated by a compacted neck, as in Fig. 5, where the length of a single bead is designated by L_B, and the length of a cylindrical neck by L_C.

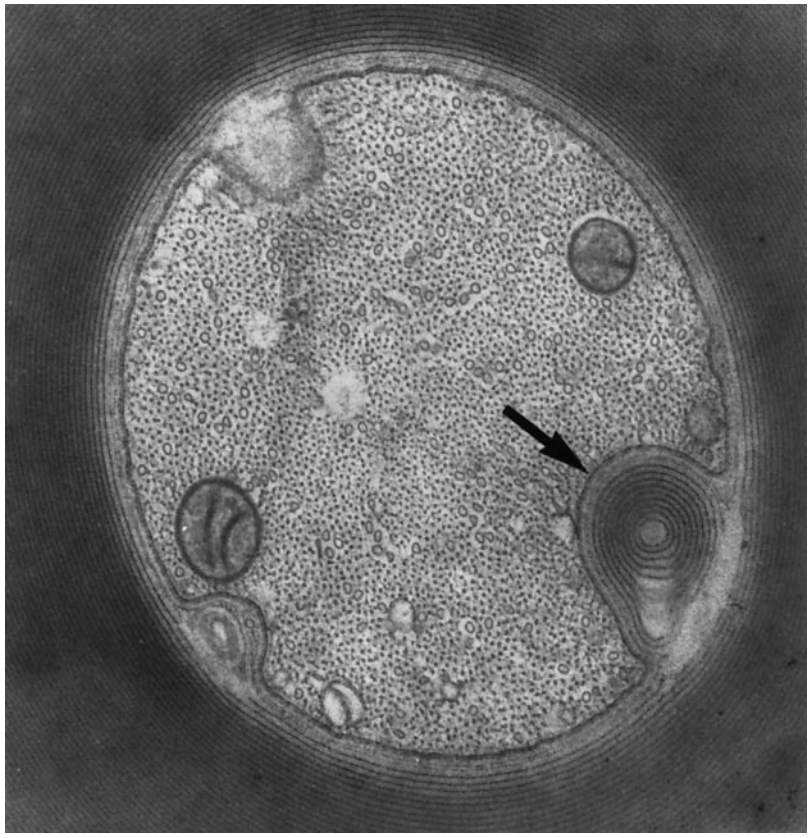

FIGURE 3 Cross section of the constriction of a beaded myelinated fiber prepared by freeze-substitution, showing the compaction of the cytoskeletal organelles within the axon. The myelin sheath, with its major dense and minor dense lines, is seen surrounding the axon. The axolemma appears as a heavier double-lined, somewhat wrinkled structure with several intrusions pushing into the axon. The arrow points to the largest of the intrusions (*arrow*), showing a laminar organization similar to that of the myelin sheath. The other intrusions are not as well formed. Within the axon the microtubules are seen as open circular structures of ~250 Å interspersed among the smaller neurofilament profiles of ~100 Å. Also present are two mitochondrial profiles. Magnification, ×63,200.

Shape of a bead

We assume that the nerve fiber has an axisymmetrical form. Because the ratio of p and γ is a constant,

$$c_0 = \frac{p}{\gamma}, \tag{2}$$

the Laplace equation can be rewritten as

$$c_m + c_p = c_0. \tag{3}$$

This equation states that the average membrane curvature should remain constant over the bead and be equal to c_0. This same equation has appeared in a paper by Deuling and Helfrich (1977), who analyzed membrane shape using spontaneous curvature c_0 rather than tension (Volkov et al., 1997).

The equation for nerve fiber contour can be presented as

$$\frac{dx}{dr} = \cot \alpha, \tag{4}$$

where the principal curvatures are

$$c_p(r) = \frac{\cos \alpha}{r} \quad \text{and} \quad c_m(r) = -\sin \alpha \frac{d\alpha}{dr}. \tag{5}$$

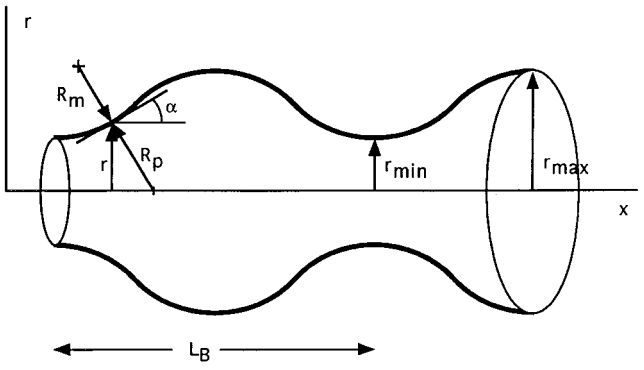

FIGURE 4 Beaded shape of a neuron and parameters describing the contour.

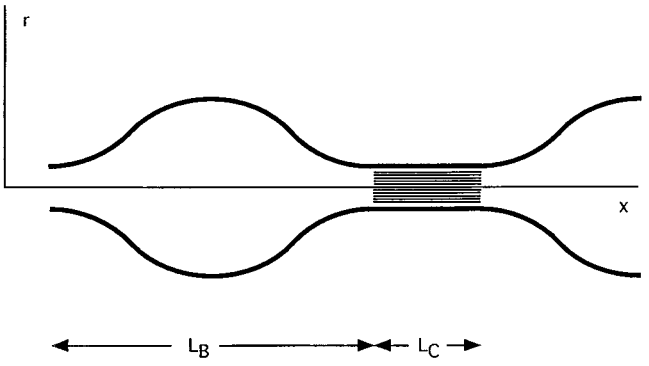

FIGURE 5 The model of beading with supported cylindrical membrane.

The average radius r_{av} of a beaded nerve fiber and the dimensionless amplitude a of contour oscillations are

$$r_{av} = \frac{r_{max} + r_{min}}{2} \quad \text{and} \quad a = \frac{r_{max} - r_{min}}{r_{max} + r_{min}}. \tag{6}$$

The shape of a bead is given by the function

$$x(r) = x(r_{min}) + r_{av}\int_{1-a}^{r/r_{av}} f(\xi)\mathrm{d}\xi, \tag{7}$$

with

$$f(\xi) = \frac{(\xi^2 + 1 - a^2)}{\sqrt{4\xi^2 - (\xi^2 + 1 - a^2)^2}}. \tag{8}$$

The shape of a bead is determined by the dimensionless amplitude a only, and the actual size of beads is defined by r_{av}. A few examples of shapes given by the function in Eq. 7 for $a = 0.2$, 0.5, and 0.9 are presented in Fig. 6. One can see that when amplitude (a) is small, the beads can be approximated by a sinusoidal function; however, as the amplitude increases, the beads become more rounded.

The shape of a compacted neck is a cylinder, as presented in Fig. 5. The length of the cylindrical neck in a dimensionless form can be designated by $g = L_C/L_B$. The radius r_C of the cylinder is equal to the minimum radius of the bead: $r_C = (1 - a)r_{av}$.

Beaded nerve fiber parameters

The length L_B of a single bead is found from Eq. 7:

$$L_B = 2r_{av}\int_{1-a}^{1+a} f(\xi)\mathrm{d}\xi. \tag{9}$$

The normalized length of a bead L_B/r_{av}, which is a function of amplitude a only, is presented in Fig. 7 *A* (*upper curve*). When a varies over its total range, from 0 to 1, the normalized length of a bead changes from 6.28 to 4.00.

When an external force transforms a nerve fiber, its volume and surface area cannot change significantly. The volume and the surface area of a single bead are

$$V_B = 2\pi r_{av}^3\int_{1-a}^{1+a} \xi^2 f(\xi)\mathrm{d}\xi, \quad A_B = 4\pi r_{av}^2\int_{1-a}^{1+a} \xi\sqrt{1 + f^2(\xi)}\mathrm{d}\xi. \tag{10}$$

The ratio of the volume to the surface area should remain the same as it was in the original nerve fiber. If the beaded nerve fiber originated from a cylinder with radius r_0, this ratio is $r_0/2$, and hence

$$r_{av} = r_0\frac{\int_{1-a}^{1+a} \xi\sqrt{1 + f^2(\xi)}\mathrm{d}\xi}{\int_{1-a}^{1+a} \xi^2 f(\xi)\mathrm{d}\xi}. \tag{11}$$

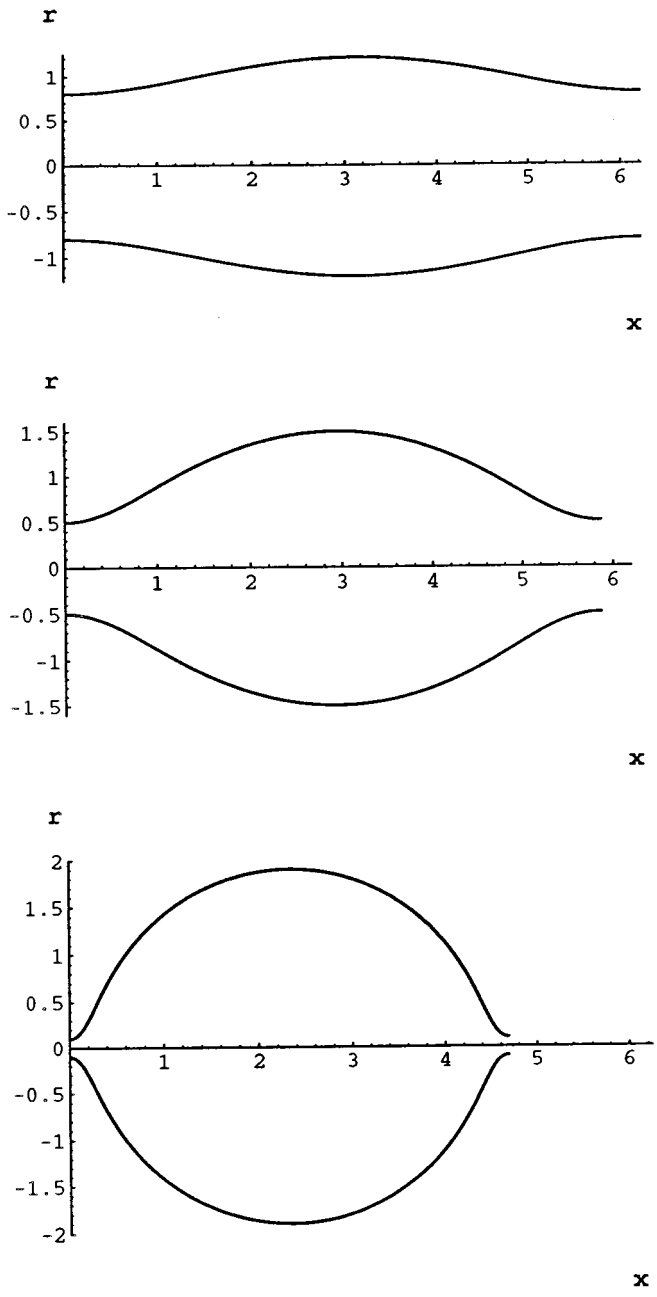

FIGURE 6 Bead shapes corresponding to the amplitude of oscillation equal $a = 0.2$, 0.5, and 0.9 (*from top to bottom*).

This equation gives the dependence of the average radius r_{av} on the amplitude of contour oscillations a (Fig. 7 *B*). As one can see, the average radius decreases with the progress of beading. Having the function in Eq. 11, one can plot the length of the bead L_B normalized by initial radius as a function of a (Fig. 7 *A*, *lower curve*). The latter curve is more useful because it employs a constant parameter for normalization, the initial radius of the neuron. Therefore, one can conclude that at small oscillations ($a \ll 1$) the bead has the length of 6.28 × (initial radius), whereas for large oscillations ($a \approx 1$) this period decreases to only 3 × (initial

radius). This variation is very clear from Fig. 6, where a changes from 0.2 to 0.9.

By excluding the average radius r_{av} from Eqs. 10 and 11, one can find final expressions for the length L_B, area A_B, and volume V_B of a bead:

$$L_B = 2r_0 \frac{[\int_{1-a}^{1+a} f(\xi)d\xi][\int_{1-a}^{1+a} \xi\sqrt{1+f^2(\xi)}d\xi]}{\int_{1-a}^{1+a} \xi^2 f(\xi)d\xi},$$

$$A_B = 4\pi r_0^2 \frac{[\int_{1-a}^{1+a} \xi\sqrt{1+f^2(\xi)}d\xi]^3}{[\int_{1-a}^{1+a} \xi^2 f(\xi)d\xi]^2}$$

$$V_B = 2\pi r_0^3 \frac{[\int_{1-a}^{1+a} \xi\sqrt{1+f^2(\xi)}d\xi]^3}{[\int_{1-a}^{1+a} \xi^2 f(\xi)d\xi]^2}. \quad (12)$$

The combination of a bead and a cylinder has the following length, surface area, and volume:

$$L_{tot} = 2(1+g)r_{av}\int_{1-a}^{1+a} f(\xi)d\xi,$$

$$A_{tot} = 4\pi r_{av}^2\left[\int_{1-a}^{1+a} \xi\sqrt{1+f^2(\xi)}d\xi + (1-a)g\int_{1-a}^{1+a} f(\xi)d\xi\right],$$

$$V_{tot} = 2\pi r_{av}^3\left[\int_{1-a}^{1+a} \xi^2 f(\xi)d\xi + (1-a)^2 g\int_{1-a}^{1+a} f(\xi)d\xi\right]. \quad (13)$$

The average radius r_{av} is found from the condition of conservation of surface area and volume ($V_{tot}/A_{tot} = r_0/2$):

$$\frac{r_{av}}{r_0} = \frac{\int_{1-a}^{1+a} \xi\sqrt{1+f^2(\xi)}d\xi + (1-a)g\int_{1-a}^{1+a} f(\xi)d\xi}{\int_{1-a}^{1+a} \xi^2 f(\xi)d\xi + (1-a)^2 g\int_{1-a}^{1+a} f(\xi)d\xi}. \quad (14)$$

This normalized average radius is a function of amplitude a and dimensionless length of the neck g.

Elongation

If all of these transformations are caused by stretching the nerve, then its length should increase with a. Therefore, the model should meet this obvious physical condition, although there is no guarantee that this is actually so. Let us consider a portion of a nerve fiber with length l_0 and membrane area $A = 2\pi r_0 l_0$. After transformation the length is

$$l = \frac{AL_{tot}}{A_{tot}}. \quad (15)$$

If the elongation is defined as $\epsilon = (l - l_0)/l_0$, then

$$\epsilon = \frac{[(1+g)\int_{1-a}^{1+a} f(\xi)d\xi]}{[\int_{1-a}^{1+a} \xi^2 f(\xi)d\xi + (1-a)^2 g\int_{1-a}^{1+a} f(\xi)d\xi]} \frac{[\int_{1-a}^{1+a} \xi^2 f(\xi)d\xi + (1-a)^2 g\int_{1-a}^{1+a} f(\xi)d\xi]}{[\int_{1-a}^{1+a} \xi\sqrt{1+f^2(\xi)}d\xi + (1-a)g\int_{1-a}^{1+a} f(\xi)d\xi]^2} - 1. \quad (16)$$

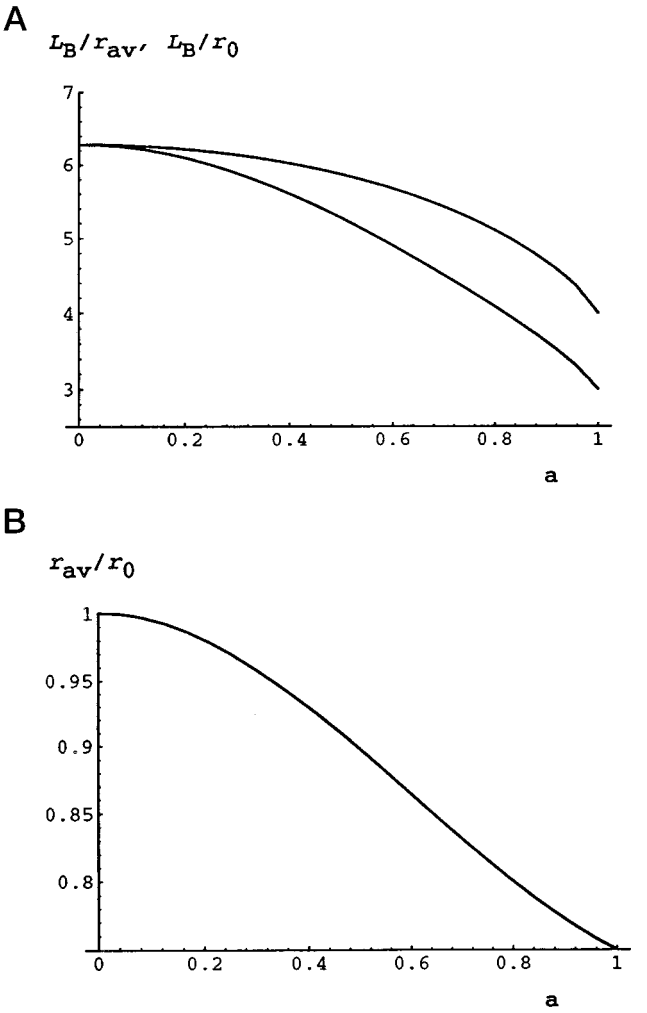

FIGURE 7 Variation of parameters of beading with amplitude of oscillations. (*A*) Period of beading L_B normalized by r_{av} (*upper curve*) and by r_0 (*lower curve*). (*B*) Average radius normalized by r_0.

Elongation ϵ is a function of the amplitude a and the length of the neck g, as presented in Fig. 8 *A*. Let us consider for the beginning a beaded fiber without necks ($g = 0$). For this case the dependence of ϵ on amplitude a is presented by the first curve from the bottom. Surprisingly enough, the whole curve finds itself below the abscissa, and hence ϵ is *negative*, which means that with the development of beads, the nerve fiber does not elongate, but rather shortens. Therefore, the application of a force should not cause beading according to this mechanism, but rather would eliminate beads that might already exist.

Appearance of a neck drastically changes the situation. When g is not equal to zero, at least a portion of the curve finds itself in the positive region. If the neck is short, only a small elongation occurs. If the neck length exceeds 0.5, the entire curve remains above zero. Interestingly enough, all of the curves that enter the positive region display a maximum, after which the elongation decreases. This means that if an external force causes the beading, then at a given neck length, the amplitude of the contour should increase

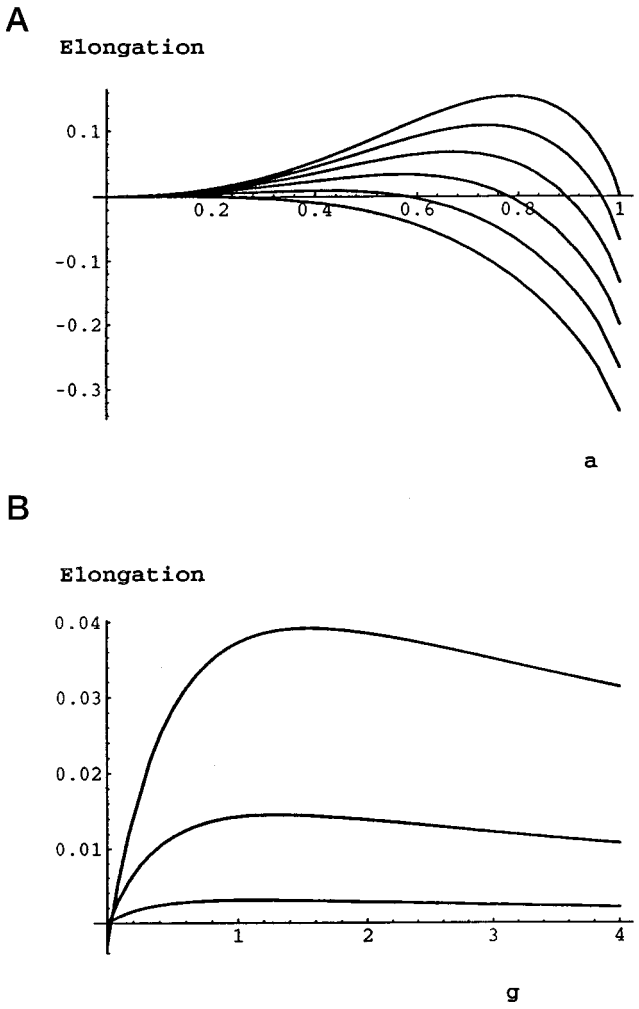

FIGURE 8 Dependence of fiber elongation ϵ on parameters of the model. (*A*) Elongation as a function of a for neck length (*from the bottom to the top*) equal to $g = 0.0$, 0.1, 0.2, 0.3, 0.4, and 0.5. (*B*) ϵ as a function of g for three values of amplitude: $a = 0.1$, 0.2, and 0.3 (*from bottom to top*).

only to a certain limit corresponding to the maximum of the curves.

Fig. 8 *B* presents elongation (ϵ) as a function of neck length (g) for three values of amplitude: $a = 0.1$, 0.2, and 0.3 (from bottom to top). In this case, the curves also exhibit a maximum, which means that neck length is restricted to certain values. For these three curves, maximum elongation occurs when g is $\sim$1, i.e., when the neck is about the length of the bead. For larger values of a the length of the neck also increases.

Specific features of myelinated fibers

Beading of myelinated and unmyelinated fibers can be universally described by the model presented above. However, in the case of myelinated fibers there are a number of important additional features that need to be considered. These relate to the phenomenon of intrusion, where an infolding of the axolemma along with more or less of the myelin sheath lamellae occurs in the beaded fibers (Ochs and Jersild, 1990). These may exhibit various shapes in a cross section of the constriction from narrow finger-like protrusions into the axon to hillocks of pillar-like structures enclosed by axolemma (Fig. 3).

All of these intrusive phenomena can be accounted for with the same model when the thickness of the myelin sheath is taken into consideration. Suppose that the outer radius of the initial nonstretched myelin fiber is r_0 and the thickness of the myelin sheath is H. After stretch, the radius of constriction is r_1, and therefore the external surface of the myelin sheath is stretched in the axial direction with coefficient $k = r_0/r_1$. This parameter exceeds 1 and can be called the coefficient of fiber compression. If myelin layers cannot slide relative to each other in the axial direction, then the whole myelin sheath is stretched with the same coefficient k. This means that the radius of the axolemma after stretching should be $(r_0 - H)/k$.

However, because the myelin sheath preserves its thickness, the radius of the axolemma is reduced from $r_0 - H$ to $r_1 - H = r_0/k - H$, i.e., to a smaller value than $(r_0 - H)/k$. Therefore, the axolemma will have extra area (per unit length) equal to

$$2\pi[(r_0 - H)/k - (r_0/k - H)] = 2\pi H(1 - 1/k), \qquad (17)$$

and the relative excess of axolemma is $\alpha = (a - 1/k)/(r_1/H - 1)$. The only way to accommodate this extra area is that the axolemma, together with more or less of the adjacent inner layers of myelin, bulges inwardly. This is exactly what is observed experimentally.

To get an idea of how large the bulging should be according to this model, let us make a few estimates. In Figure 8 *A* of Ochs et al. (1997), the ratio r_1/H is $\sim$2.65. Assuming that the initial fiber was compressed to one-half of its thickness, the extra area rises to 40%.

This extra area should go to infoldings, hillocks, or spherical intrusion bodies. In figure 7 of Ochs et al. (1997), the area of intrusions constitutes $\sim$43% of the circumference of the axon, whereas in their figure 8 *A* it is $\sim$15%. These experimental observations fit the model estimates reasonably well.

DISCUSSION

The beaded neurites seen in cultured DRG neurons when stretched closely resemble beaded myelinated fibers and the axons of unmyelinated fibers in mildly stretched mammalian nerves. In both cases, the degree of lengthening needed to bead the axons is very small. Similarly, in the case of peripheral nerves, after the zig-zag course of the fibers is straightened, the degree of stretch needed to transform the fibers from their essentially cylindrical shape into the beaded form also amounts to only several percent (Pourmand et al., 1994).

The basic proposition of the model is that the membrane is free to become deformed under the influence of tension and hydrostatic pressure, whereas volume and surface area remain constant. This was supported by experimental observation of myelinated fibers with sufficiently reduced axonal volume, as occurs in hibernating frogs. In this case the fibers did not bead when their nerves were stretched (Ochs, 1965). A failure of fibers to bead on stretch was also seen in rat nerves after they were placed in a hypertonic medium to cause a reduction of their axonal volume (unpublished experiments).

In the normovolemic fibers the sinusoidal shape of beading comes about by the movement of axonal fluid and soluble substances from the constricted regions into the adjoining regions, causing the latter to swell beyond their normal diameter (Ochs et al., 1994).

In considering the fundamental position of the continuum model of the existence of membrane with constant area and a constant volume of the axon, the objection might be raised that the plasmalemma has folds and that stretching would straighten them out. However, in cross section and in longitudinal electron microscopic sections, no such folds were seen. In these sections the magnifications used for the electron microscopic studies were such that folds as small as the thickness of the membrane, ~80 Å, could be observed if such were present. This applies to the plasmalemma of myelinated and unmyelinated fibers and to the membranes constituting the lamellae of myelin sheath of myelinated fibers.

Compaction of the cytoskeletal microtubules and neurofilaments in the constriction regions has been shown for both myelinated (Figures 8 and 9 of Ochs and Jersild, 1987) and unmyelinated axons (Figures 2 and 3 of Ochs et al., 1996). An interesting phenomenon occurs at the region of constriction of myelinated nerves, where the degree of constriction is limited by the compacted cytoskeleton within the axon. In particular, in the more extreme beaded forms showing hyperbeading, the constricted cylindrical region becomes even more elongated. This results in the movement of more fluid into the expanded regions, making them appear more globular (Figure 5 of Pourmand et al., 1994). When the cytoskeleton is degraded by exposure to β,β'-iminodipropionitrile (IDPN), the constriction process can rapidly go further, to the point where, within hours, the membranes merge to close off and form ovoids similar in form to those that develop days later in the course of Wallerian degeneration (Ochs et al., 1996).

The general theoretical model includes, as a special case, these intrusions seen in beaded myelinated fibers, where some of the myelin of the sheath enters along with the infolded axolemma in the constricted axons (Ochs and Jersild, 1990). These observations, and as well the sausage-shaped and ovoid forms, which deviate from the smooth undulations seen when the cytoskeleton is degraded by IDPN, led to the concept that a special mechanism involving the spectrin and actin of the membrane skeleton affixed to the inner face of the axolemma, brings about the beading constrictions (Ochs et al., 1996).

A brief discussion of the role of beading in normal nerve physiology is in order. In the peripheral nerve there are protections against stretching the fibers to the point where beading occurs. Within the sheaths the fibers have zig-zag disposition. On stretch the fibers straighten out, and at that point a very small tension will convert the cylindrical fibers to the beaded form. Further extension is restrained by the collagen fibers parallel to the nerve fibers. This shape transformation occurs quickly and is quickly reversed on relaxation. In hyperextension of a limb, the fibers of nerves so extended were shown to become beaded (Ochs et al., 1997).

This mechanism is regarded as accounting not only for the beading elicited by stretch, but by other agents: hypoxia, the action of toxins, or transection leading to Wallerian degeneration form changes appearing in cultured neurites as well as in peripheral nerve fibers (Ochs et al., 1997). A noxious intervention may not even be needed to elicit beading. Beaded nerve fibers have been seen within the mammalian central nervous system, in the dorsal columns of the spinal cord and cortex, and in *Aplysia*, where there was no imposition of stretch (Ochs et al. 1997; Allen et al., 1997; Zhu et al., 1997). These observations indicate that some process in the neuron can engage the membrane mechanism responsible for beading, even in normal fibers, and point to the need for further investigation and analysis of the beading phenomenon in light of its possible functional role.

Our experiments and model suggest that nerve fiber shape transformation of small-diameter nerve fibers (A-delta or C) and fine dendritic processes or "free" nerve endings can have a functional significance related to specific properties of nerve impulse conduction in nonuniform fibers, as described in a previous paper by Tanelian and Markin (1997).

We thank Mrs. Vera McAdoo of the Department of Anatomy, Indiana University School of Medicine, for assistance with the electron micrographs.

This work was supported by the J. F. Maddox Foundation (DLT).

REFERENCES

Allen, B. J., S. D. Rogers, J. R. Ghilardi, P. M. Menning, M. A. Kuskovsky, I. Basbaum, D. A. Simone, and P. W. Mantyh. 1997. Noxious cutaneous thermal stimuli induce a graded release of endogenous substance P in the spinal cord: imaging peptide action *in vivo*. *J. Neurosci.* 17:5921–5927.

Bar-Ziv, R., and E. Moses. 1994. Instability and "pearling" states produced in tubular membranes by competition of curvature and tension. *Phys. Rev. Lett.* 73:1392–1395.

Deuling, H. J., and W. Helfrich. 1991. A theoretical explanation of the myelin shapes of red blood cells. *Blood Cell.* 3:713–720.

Elgsaeter, A., B. Y. Stokke, A. Mikkelsen, and O. Branton. 1986. The molecular basis of erythrocyte shape. *Science.* 234:1217–1223.

Mantyh, P. W., C. J. Allen, and J. R. Ghilardi, et al. 1995a. Rapid endocytosis of a G protein-coupled receptor: substance P-evoked internalization of its receptor in the rat striatum *in vivo*. *Proc. Natl. Acad. Sci. USA.* 92:2622–2626.

Mantyh, P. W., E. DeMaster, A. Malhotra, J. R. Ghilardi, S. D. Rogers, C. R. Mantyh, H. Liu, I. Basbaum, S. R. Vigna, J. E. Maggio, and D. A.

Simone. 1995b. Receptor endocytosis and dendrite reshaping in spinal neurons after somatosensory stimulation. *Science.* 268:1629–1632.

Ochs, S. 1965. Beading of myelinated nerve fibers. *Exp. Neurol.* 12:84–95.

Ochs, S., and R. A. Jersild, Jr. 1987. Cytoskeletal organelles and myelin structure of beaded nerve fibers. *Neuroscience.* 22:1041–1056.

Ochs, S., and R. A. Jersild, Jr. 1990. Myelin intrusions in beaded nerve fibers. *Neuroscience.* 36:553–567.

Ochs, S., R. A. Jersild, Jr., R. Pourmand, and C. G. Potter. 1994. The beaded form of myelinated nerve fibers. *Neuroscience.* 61:361–372.

Ochs, S., R. Pourmand, and R. A. Jersild, Jr. 1996. Origin of beading constrictions at the axolemma: presence in unmyelinated axons and after β,β'-iminodipropionitrile (IDPN) degradation of the cytoskeleton. *Neuroscience.* 70:1081–1096.

Ochs, S., R. Pourmand, R. A. Jersild, Jr., and R. N. Friedman. 1997. The origin and nature of beading: a reversible transformation of the shape of nerve fibers. *Prog. Neurobiol.* 52:391–426.

Pourmand, R., S. Ochs, and R. A. Jersild, Jr. 1994. The relation of the beading of myelinated nerve fibers to the bands of Fontana. *Neuroscience.* 61:373–380.

Tanelian, D. L., and V. S. Markin. 1997. Biophysical and functional consequences of receptor-mediated nerve fiber transformation. *Biophys. J.* 72:1092–1108.

Volkov, A. G., D. W. Deamer, D. L. Tanelian, and V. S. Markin. 1997. Liquid Interfaces in Chemistry and Biology. John Wiley and Sons, New York.

Wang, Z., R. J. Van den Berg, and D. L. Ypey. 1994. Resting membrane potentials and excitability at different regions of dorsal root ganglion neurons in culture. *Neuroscience.* 60:245–254 (Abst.).

Zhu, H., S. Wu, and S. Schachter. 1997. Site-specific and sensory neuron-dependent increases in postsynaptic glutamate sensitivity accompany serotonin-induced long-term facilitation at *Aplysia* sensomotor synapses. *J. Neurosci.* 17:4976–4985.